Testing Supersymmetric Theories at Linear e^+e^- Colliders

Keisuke Fujii

National Laboratory for High Energy Physics (KEK), Tsukuba, Ibaraki 305, Japan

Tests of supersymmetric theories at future linear e^+e^- colliders are discussed from experimental point of view. The experimental procedures to determine the masses and mixings of SUSY particles through the measurements of various differential cross sections are explained, where the power of polarized electron beam is stressed. The implications of the so determined SUSY breaking parameters are discussed in relation to the GUT scale physics.

1 Introduction

The existence of at least one light neutral Higgs boson is one of the most important predictions of low energy supersymmetry (SUSY). Its discovery alone is, however, not enough to prove supersymmetry. It is definitely necessary to find *at least* one supersymmetric particle (sparticle) to show that there is indeed SUSY in nature. Once a sparticle is found, what else can we do? Well, it is only the beginning at a future linear e^+e^- collider. True excitements come after this, which are the studies on the supersymmetry breaking (sbreaking) sector determined presumably by GUT or Planck scale physics. The sbreaking sector fixes masses and mixings of sparticles, which, in turn, determine various differential cross sections. We can thus determine masses and mixings of sparticles through the measurements of various differential cross sections, thereby testing SUSY quantitatively and uncovering the structure of the sbreaking sector.

In this talk, I will demonstrate how well we can do this at a future linear e^+e^- collider, taking a sample case.

2 SUSY Study Scenario

It is well known that mass relations derived through renormalization group equations (RGE) from GUT and common scalar mass hypotheses lead us to a general conclusion: colorless sparticles are lighter than colored ones and right-handed sfermions are lighter than left-handed ones. Thus the first SUSY particle (FSP) is most likely to be either the lighter chargino ($\tilde{\chi}_1^\pm$) or the right-handed sleptons ($\tilde{l}_R^\pm$).

The following parameter set: $(m_0, M_2, \mu, \tan\beta) = (70\ \mathrm{GeV}, 250\ \mathrm{GeV}, 400\ \mathrm{GeV}, 2)$, which we will use in what follows unless otherwise stated, gives the following sparticle mass spectrum:

$$\begin{aligned}(m_{\tilde{\chi}_1^0}, m_{\tilde{\chi}_2^0}, m_{\tilde{\chi}_1^\pm}, m_{\tilde{l}_R}, m_{\tilde{l}_L}, m_{\tilde{\nu}_L}) \\ = (118, 222, 220, 142, 236, 227)\ \mathrm{GeV}.\end{aligned}$$

Thus our FSP will be the right-handed sleptons pair-produced in e^+e^- collisions. Let us now start looking at how a typical SUSY scenario goes at the linear collider[1].

2.1 *Study of $\tilde{l}_R^\pm (l \neq \tau)$*

Since a right-handed slepton decays directly into a lepton plus an LSP, the signal to look for is an acoplanar lepton pair: $e^+e^- \to \tilde{l}_R^+\tilde{l}_R^- \to l^+\tilde{\chi}_1^0 l^-\tilde{\chi}_1^0$. On the other hand, the background to this reaction is standard model (SM) processes with neutrinos which mimic the LSP. The key point here is the power of a highly polarized electron beam available only at linear colliders. For instance, we can eliminate the largest SM background ($e^+e^- \to W^+W^-$ with $W \to l\nu$) very effectively, using a right-handed electron beam: the transverse W-pair production vanishes in the symmetry limit since the s-channel diagram involves a W^0 and the t-channel diagram exchanges a ν_e, both of which only couple to left-handed electrons. On the other hand, the signal cross section will be enhanced because of the weak hypercharge difference between e_L^- and e_R^-: $\sigma_R = 4\sigma_L$ in the symmetry limit. We can see this clearly in Fig. 1, which plots

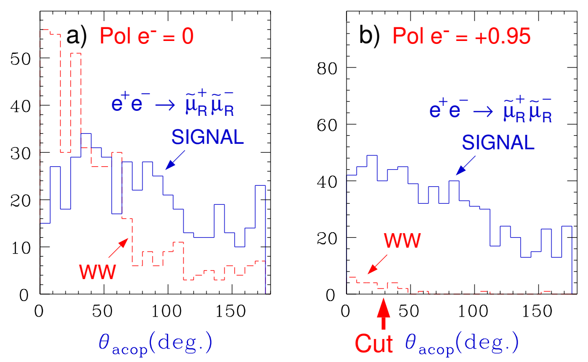

Figure 1: Examples of acoplanarity distributions for smuon pair productions with (a) an unpolarized beam and (b) a 95 %-right-handed polarized beam. The Monte Carlo data correspond to an integrated luminosity of 20 fb^{-1} at $\sqrt{s} = 350$ GeV.

the acoplanarity distributions for smuon pair production with and without the right-handed electron beam. The requirement of $\theta_A > 30°$ eliminates the background to a negligible level, providing us with a very clean sample for precision studies.

Using this clean sample, we can determine the masses of the LSP and the right-handed slepton through the measurement of the final-state lepton energy distribution (see Fig. 2-a)): the end points of this distribution are kinematically fixed by the LSP and the slepton masses. A two-parameter fit to this distribution gives a contour plot shown in Fig. 2-b), which tells us that we can determine these masses to a 1% level.

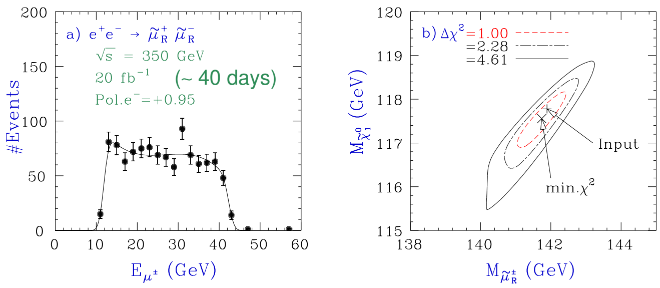

Figure 2: (a) Energy distribution of muons from smuon decays for the same Monte Carlo parameters as with Fig.1-b). The solid line corresponds to the best fit curve, letting $m_{\tilde{\mu}_R}$ and $m_{\tilde{\chi}_1^0}$ move freely. (b) Contours in the $m_{\tilde{\mu}_R}$-$m_{\tilde{\chi}_1^0}$ plane obtained from the fit to the energy distribution.

With the right-handed selectron and smuon masses determined this way, we can make a test of generation independence of sfermion masses. The hidden sector SUSY breaking implies the universality of scalar masses at the GUT scale, which leads to the mass degeneracy of the first and the second generations. Fig. 3 is an example of the test of the generation independence, demonstrating potential precision available at the future linear collider.

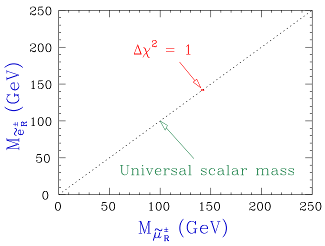

Figure 3: The expected $\Delta\chi^2 = 1$ contour in the $m_{\tilde{\mu}_R}$-$m_{\tilde{e}_R}$ plane.

Now that we know the LSP and the slepton masses, we can solve kinematics up to 2-fold ambiguities. Fig. 4-a) plots the two solutions for the cosine of the smuon production angle. Comparison of this with the corresponding generated one (histogram) suggests that the wrong solution makes a flat background. After the background subtraction, we get the plot in Fig. 4-b), which shows a $\sin^2\theta$ distribution characteristic of s-channel pair productions of a spinless particle. In this way we can confirm that our smuon is really a scalar particle.

On the other hand, the right-handed selectron pair production has t-channel neutralino-exchange diagrams in addition. Notice that only their bino ($\tilde{B}$) components contribute here, which will produce a forward peak if significant. Figs. 4-c) and -c) are similar plots to Figs. 4-a) and -b) for the right-handed selectron pair production. The forward peak indicates that our LSP is bino-dominant.

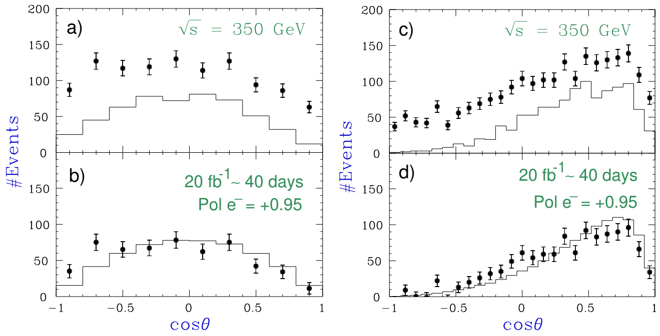

Figure 4: (a) Production angle distribution of $\tilde{\mu}_R^-$ with respect to the electron beam axis. The points with error bars are the distribution of the two solutions reconstructed from the selected sample corresponding to Fig. 2-a). The histogram is the generated $\cos\theta$ distribution for the selected sample. (b) Production angle distribution after the background subtraction compared with the scaled generated distribution before selection cuts. No acceptance correction is applied to the reconstructed distribution. (c) and (d): Similar plots to Fig. 4-(a) and -(b) for $e^+e^- \to \tilde{e}_R^+\tilde{e}_R^-$.

2.2 $\tilde{\tau}^\pm$ Study

Stau decays provide another handle to uncover the nature of the LSP through the measurement of the final state tau polarization [2]. For simplicity, let us assume that $\tilde{\tau}_L$-$\tilde{\tau}_R$ mixing is negligible and the lighter stau is essentially $\tilde{\tau}_R$. If the LSP is bino-dominant ($\tilde{\chi}_1^0 \simeq \tilde{B}$), the final-state tau will be right-handed ($\tilde{\tau}_R^- \to \tau_R^- \tilde{\chi}_1^0$), since the $\tilde{\tau}\tilde{\chi}_1^0\tau$ coupling stems from the gauge coupling, which is chirality-conserving. On the other hand, if the LSP is higgsino-dominant ($\tilde{\chi}_1^0 \simeq \tilde{H}_1^0$), the $\tilde{\tau}\tilde{\chi}_1^0\tau$ coupling will be of Yukawa type and chirality-flipping, thereby resulting in a left-handed tau in the final state. We can thus determine the nature of the LSP by measuring the final-state tau polarization. Figs. 5-a) and -b) shows examples of such a measurement for the bino- and higgsino-dominant cases, respectively. It should be emphasized that this measurement is unique to the stau decays. From the figures, we can see that $\Delta P_\tau \simeq 0.1$ is quite feasible, given an integrated luminosity of 100 fb^{-1}.

2.3 Study of $\tilde{\chi}_1^\pm$

From the slepton studies, we can determine the mass of the LSP($\tilde{\chi}_1^0$) to better than 1 %. From this we can set

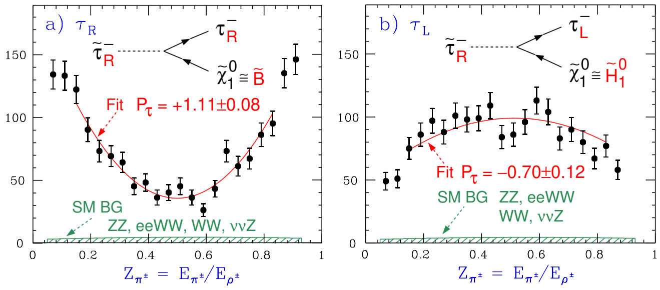

Figure 5: Distributions of the $\pi^\pm$ energy fraction with respect to the energy of the $\rho^\pm$ from $\tau \to \nu_\tau \rho$ decays for (a) bino-dominant and (b) higgsino-dominant LSP cases. The points with error bars are the Monte Carlo data corresponding to 100 fb^{-1} with $P_{e^-} = +0.95$ at $\sqrt{s} = 500$ GeV, where $m_{\tilde\tau} = 150$ GeV, $m_{\tilde\chi_1^0} = 100$ GeV, and $\sigma_{\tilde\tau\tilde\tau} = 100$ fb are assumed. The shaded histograms are the expected standard-model backgrounds from $e^+e^- \to ZZ, W^+W^-$, $e^+e^-W^+W^-$, and $\nu\bar\nu Z$.

an upper limit on the lighter chargino mass, assuming the GUT relation among the gaugino mass parameters. This upper limit corresponds to the gaugino-dominant case ($m_{\tilde\chi_1^\pm} \simeq 2 \times m_{\tilde\chi_1^0}$), while the LSP and the lighter chargino will be almost mass-degenerate in the higgsino-dominant case.

We thus set our center of mass energy just above $4 \times m_{LSP}$ and look for $\tilde\chi_1^\pm$ pair productions. In our sample case, the chargino decays into a real W and an LSP ($\tilde\chi_1^\pm \to W^\pm \tilde\chi_1^0$). The signal to look for will thus be an acoplanar W pair in 4-jet final states. Fig. 6 shows the acoplanarity angle distribution for the signal events (solid histogram) together with major standard-model backgrounds. A cut at $\theta_A = 30°$ will give us a fairly

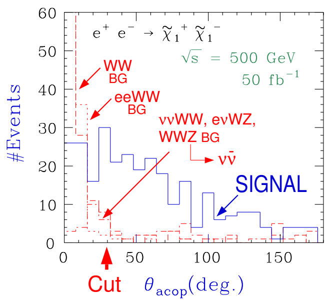

Figure 6: Acoplanarity angle distribution for $e^+e^- \to \tilde\chi_1^+\tilde\chi_1^-$ together with major standard-model backgrounds.

clean sample for precision studies.

As we did to the sleptons, we can first use this clean sample to determine the chargino mass. This time, what we should look at is the energy distribution of the final-state W's from chargino decays. A 2-parameter fit letting $m_{\tilde\chi_1^\pm}$ and $m_{\tilde\chi_1^0}$ move freely allows us to determine the chargino mass to $\Delta m_{\tilde\chi_1^\pm} \simeq 8$ GeV. If we use the LSP mass constraint from the slepton study, we can improve this to $\Delta m_{\tilde\chi_1^\pm} \simeq 5$ GeV.

Using the clean sample, we can also measure the production cross section. Notice that, for the right-handed electron beam, only higgsino components contribute to the chargino pair production in the symmetry limit, since the gauge boson exchanged in the s-channel is B ($U(1)_Y$ gauge boson), which does not couple to wino components. By measuring the production cross section for the right-handed electron beam, we can thus determine the composition of $\tilde\chi_1^\pm$.

We now know the LSP ($\tilde\chi_1^0$) and the chargino ($\tilde\chi_1^\pm$) masses, which constrain the chargino and neutralino mass matrices, the production cross section for $e^+e^-_R \to \tilde e^+_R \tilde e^-_R$, which depends on the bino component of the LSP, and the production cross section for $e^+e^-_R \to \tilde\chi_1^+\tilde\chi_1^-$, which provides information on the chargino composition. Combining these measurements together, we can carry out a global fit to determine sbreaking parameters: $(M_1, M_2, \mu, \tan\beta)$. Notice that we did not assume the GUT relation between M_1 and M_2 here, since this is what we want to test now. Fig. 7 is the result from such a global fit to Monte Carlo data generated with the GUT relation indicated as a dashed line. In this way, we can test the GUT relation.

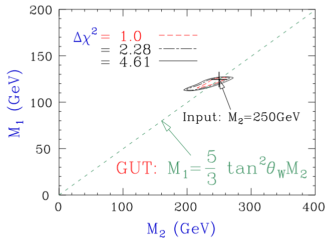

Figure 7: Constant χ^2 contours in the M_2-M_1 plane obtained from the global fit explained in the text. The dotted line shows the GUT relation.

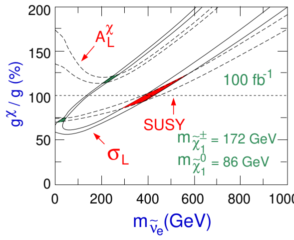

Figure 8: Limits on $(m_{\tilde\nu}, g^\chi/g)$ from σ_L and A_L^χ with 100 fb^{-1}. Parameters are $(M_2, \mu, m_{\tilde l}, m_{\tilde q})$ = $(170, -500, 400, 700)$ GeV and $\tan\beta = 4^3$.

So far, we have been assuming SUSY, being satisfied with a qualitative test of SUSY (the existence of a new particle consistent with sparticle interpretation). At this point, we can even try to test SUSY quantitatively[3]. In general SUSY relates mutually supersymmetric couplings: $e_L \tilde W \tilde\nu$ and $e_L W \nu$ for instance. This relation can be cast into the form $g = g^\chi$, where g represents the $SU(2)_L$ gauge coupling. For simplicity, let us consider a gaugino-dominant $\tilde\chi_1^\pm$ and assume that the chargino mixing is negligible. Then the free parameters that enter the differential cross section for a left-handed electron beam are essentially $m_{\tilde\nu}$ and g^χ, since we already know $m_{\tilde\chi_1^\pm}$. In order to determine these two unknown parameters, we can use the production cross section (σ_L) and the forward backward asymmetry (A_L^χ)[a] for the left-handed elec-

[a] We cannot measure A^χ directly. There is, however, a strong correlation between the asymmetry of $\tilde\chi_1^-$ and that of W^-. We

tron beam. Fig 8 shows the constraints from the σ_L and A_L^χ measurements on the two unknown parameters. The horizontal dotted line indicates the SUSY prediction.

Once we are convinced with SUSY, we can tell the sneutrino mass from this figure. Using this and the following model-independent inequality

$$m^2_{\tilde{e}^\pm_L} \leq m^2_{\tilde{\nu}_e} + 0.77 m_Z^2,$$

we can set an upper limit on the left-handed selectron mass. Let us now look for the left-handed selectron in $e^+e^-_R \rightarrow \tilde{e}^+_L \tilde{e}^-_R$.

2.4 $\tilde{e}^\pm_L$ Study

The associate production of $\tilde{e}_L$ with $\tilde{e}_R$ proceeds via t-channel exchange of neutralinos, to which only the $\tilde{B}$ components contribute. The signal for this process is an acoplanar e^+e^- pair. When we use the right-handed electron beam to suppress standard-model backgrounds, the major background is our previous signal: $e^+e^-_R \rightarrow \tilde{e}^+_R \tilde{e}^-_R$. Notice that the use of the right-handed electron beam selects the e^+ in the final state as a carrier of the $\tilde{e}_L$ information. Fig. 9 plots the final-state electron energy against that of the positron, clearly demonstrating this fact. Projecting this to the E_{e^+} axis, we obtain a similar plot to Fig. 2-a), from which we can extract the sparticle masses as before to an accuracy better than 1 %.

Knowing both the right-handed and left-handed selectron masses enables us to make another test of the universal scalar mass hypothesis. The squared mass difference of the right-handed (belonging to $\mathbf{5}^*$) and left-handed (belonging to $\mathbf{10}$) selectrons is related to the gaugino mass parameter (M_2) through the following scalar mass formula:

$$m^2_{\tilde{e}_L} - m^2_{\tilde{e}_R} = m^2_{0(\mathbf{5})} - m^2_{0(\mathbf{10})} + 0.5 M_2^2 - 0.04 m_Z^2 \cos 2\beta.$$

The universal scalar mass hypothesis implies the representation independence ($m_{0(\mathbf{5})} = m_{0(\mathbf{10})}$), which can be tested as shown in Fig. 10: compare the $\Delta\chi^2 = 1$ contour with the prediction of the universal scalar mass hypothesis (dashed lines for $\tan\beta = 0$ and 30). Notice that the last term ($\tan\beta$-dependent term) of the above equation is small and only makes slight difference, allowing us a clean test of the representation independence.

Once the GUT relation is confirmed and the universal scalar mass hypothesis is verified in the slepton sector, we can set, with confidence, the next target energy for $\tilde{q}$ pair production. It has been demonstrated that precision mass determinations of 1 % level are also possible for squarks, even if they cascade-decay[4]. We will thus be able to test various mass relations with stronger constraints.

can measure the latter using lepton+2-jet final states.

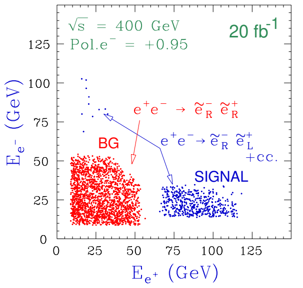

Figure 9: Distribution of final-state electron energy against that of the positron for $e^+e^-_R \rightarrow \tilde{e}^+_L\tilde{e}^-_R$ (signal) and $\tilde{e}^+_R\tilde{e}^-_R$ (background) at $\sqrt{s}$ = 400 GeV with an integrated luminosity of 20 fb^{-1}.

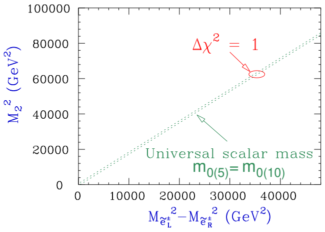

Figure 10: $\Delta\chi^2 = 1$ contour from the selectron mass measurements, compared with the prediction from the universal scalar mass hypothesis, indicated as dotted lines for $\tan\beta = 0$ and 30.

3 Summary and Conclusion

Main features of a typical SUSY scenario at a future linear e^+e^- collider can be summarized as follows. (1) The polarized electron beam will be essential to suppressing various backgrounds and to sorting out sparticle mixings. (2) The first sparticle alone will provide enough information to decide where to go for the next. (3) We can make precision measurements of masses, mixing angles, and couplings, which allow us to test key assumptions of supergravity models such as GUT relations, the hidden-sector SUSY-breaking (universal scalar mass), etc.

We can conclude that the future linear e^+e^- collider will enable us to take a first realistic step towards the GUT/Planck scale physics, once a sparticle is found there.

Acknowledgments

The author wishes to thank all the members of the JLC working group for useful discussions and comments. In particular, S. Murayama, M. Nojiri, Y. Okada, T. Tsukamoto, M. Yamaguchi deserve special mention, since most of the materials presented here are based on the collaboration with them. The author is very grateful to J. Feng, K. Hikasa, T. Kon, M. Jimbo, M. Peskin, Z. Tata and P. Zerwas for valuable discussions.

References

1. T. Tsukamoto, K. Fujii, H. Murayama, M. Yamaguchi, and Y. Okada, *Phys. Rev.* **D51** (1994) 3153.
2. M. Nojiri, *Phys. Rev.* **D51** (1995) 6281;M. Nojiri, K. Fujii, and T. Tsukamoto, in preparation.
3. J. Feng, M. Peskin, H. Murayama, and X. Tata, *Phys. Rev.* **D52** (1995) 1418.
4. J. Feng and D. Finnell, *Phys. Rev.* **D49** (1994) 2369.